International Journal of Disaster Risk Reduction 147 (2026) 106548



Contents lists available at ScienceDirect

International Journal of Disaster Risk Reduction

journal homepage: www.elsevier.com/locate/ijdrr



3D property-level flood risk visualisation for urban flood risk communication: A case study of Te Auaunga, Auckland

Fatemeh Kaleshani [a,*], Mostafa Babaeian Jelodar [a], Farzad Piadeh [b], Suzanne Wilkinson [c], Bruce Balaei [d]

[a] School of Built Environment, Massey University, Auckland, 0632, New Zealand
[b] Centre for Engineering Research, School of Physics, Engineering, Computer Science, University of Hertfordshire, AL10 9AB, UK
[c] Faculty of Design & Creative Technologies, Auckland University of Technology, Auckland, 1010, New Zealand
[d] Healthy Water and Flood Resilience Departments, Auckland Council, Auckland, 1142, New Zealand

ARTICLE INFO

Keywords:
3D flood visualisation
Risk perception
Risk communication
Risk management

ABSTRACT

Flood risk communication requires methods that translate technically robust flood information into spatial representations that can be interpreted in relation to buildings, roads, and other urban assets. Existing 3D visualisation approaches are often technically sophisticated but are not consistently demonstrated for routine GIS practice, while other approaches emphasise public engagement without documenting a GIS-based workflow. This study develops a documented GIS-based workflow for three-dimensional flood visualisation in an urban fluvial setting. The framework integrates LiDAR-derived terrain and building information with two forms of flood-depth data: indicative terrain-driven hydrologic surfaces generated using ArcHydro and authoritative hydraulic model outputs supplied by Auckland Council. These datasets are translated into neighbourhood- and property-scale 3D visualisations incorporating building exposure, road impacts, severity-based asset information, and potentially safe areas. The workflow is demonstrated for Te Auaunga, Auckland, New Zealand, and evaluated by nine professionals with experience in flood risk management, GIS, or related fields. Expert responses indicated high perceived understandability and stability (mean = 4.56 for both), together with favourable assessments of plausibility and practical usefulness. Hydrologic and hydraulic outputs showed different visual characteristics, with terrain-driven surfaces producing smoother inundation patterns and hydraulic outputs retaining greater local spatial variability. The findings support the feasibility of integrating heterogeneous flood-depth datasets and urban assets within a standard GIS environment, offering a practical complement to existing flood-information platforms. The present assessment represents an initial professional evaluation of the framework; direct evaluation with non-technical community users is required before conclusions can be drawn regarding public risk perception.

1. Introduction

Flood disasters increasingly threaten communities, infrastructure, and essential services, reinforcing the need for flood risk information that is both technically credible and readily interpretable [1,2]. Flood risk maps are widely used to communicate potential

* Corresponding author.
E-mail address: f.kaleshani@massey.ac.nz (F. Kaleshani).

https://doi.org/10.1016/j.ijdrr.2026.106548
Received 1 April 2026; Received in revised form 29 October 2026; Accepted 2 November 2026
Available online 2 November 2026
2212-4209/© 2026 Published by Elsevier Ltd. This is an open access article under the CC BY-NC-ND license (http://creativecommons.org/licenses/by-nc-nd/4.0/).

inundation, support preparedness, and inform planning and emergency-management decisions [3–5]. Their communication value, however, depends not only on the accuracy of the underlying flood information but also on whether users can relate mapped flood extent and depth to familiar buildings, roads, and neighbourhoods [4,6,7]. This has encouraged the development of visualisation techniques that use colour, symbolisation, depth cues, overlays, and interactive spatial representations to make hazard information more interpretable for different audiences [8–12].

Among the tools most widely applied for this purpose are conventional two-dimensional flood maps, which remain practical and cost-effective for technical analysis, planning, and flood risk management. However, their plan-view representation can be less intuitive for non-technical audiences, who must translate flood boundaries and depth classes into potential consequences for properties, transport routes, and surrounding infrastructure [3,4,13]. Difficulties in interpreting cartographic conventions or relating abstract hazard information to familiar physical environments can contribute to misunderstanding of underlying flood conditions [14–16]. Three-dimensional visualisation has therefore been increasingly explored as a means of placing flood information within a more recognisable spatial and built-environment context.

Existing 3D flood-visualisation approaches differ substantially in their technical architecture, intended users, and implementation requirements. Web-based systems can broaden access to interactive flood information and facilitate spatial exploration, but their implementation may depend on custom interfaces, data-delivery infrastructure, and specialised development processes [13,17,18]. Virtual- and augmented-reality applications can provide immersive and place-based representations, although they may require specialist hardware, software-development expertise, and purpose-built applications [19–22]. These technologies offer strong representational capability, but visual realism or immersion should not be assumed to improve risk understanding unless communication outcomes are directly evaluated.

Digital-twin environments further extend the integration of terrain, infrastructure, model outputs, and potentially dynamic data streams [23,24]. However, such systems can require substantial data integration, computational resources, and system architecture. Similarly, studies combining visualisation with numerical modelling, physics-based simulation, optimisation frameworks, artificial intelligence, or other analytical approaches increase technical capability but also introduce additional modelling and integration requirements [25–27]. These developments advance flood representation and analysis, yet they do not necessarily resolve the practical challenge of transforming routinely available flood-depth outputs into consistent, interpretable, and asset-referenced 3D information within standard GIS workflows.

Participatory and stakeholder-oriented approaches address a complementary dimension of flood risk communication by emphasising shared interpretation and the incorporation of stakeholder or community perspectives. These approaches involve decision-makers, emergency operators, field engineers, and other stakeholders in interpreting and communicating flood information [23,27–29]. A smaller body of research explicitly incorporates public risk perception and participatory processes, recognising the importance of community understanding, values, and lived experience [30–32].

However, these studies often emphasise engagement and qualitative interpretation rather than documenting transferable technical workflows for converting existing flood-model outputs into asset-referenced 3D visualisations. Conversely, technically sophisticated visualisation studies may demonstrate detailed flood representation without directly evaluating interpretation by non-technical users [5,20,22,33–35]. Taken together, these studies indicate that technical sophistication, participatory communication, and routine GIS implementation are not consistently integrated within a single workflow.

This gap is particularly relevant to urban fluvial flooding. Several 3D applications have focused on coastal flooding or storm-surge inundation [36–38], whereas urban riverine flooding is shaped by terrain, valley morphology, transport corridors, bridges, buildings, and connected overland flow pathways [39,40]. In such settings, displaying flood extent alone may not be sufficient for interpreting practical impacts. Users may also need to identify which buildings are exposed, how flood depth varies among properties, where road access may be disrupted, and which locations remain outside the modelled flood extent. Existing studies demonstrate the value of 3D representation, but the integration of heterogeneous flood-depth rasters, terrain data, building geometries, roads, bridges, and asset-level impact indicators within a documented GIS-native workflow remains less consistently addressed [3,5,17,41].

The research gap addressed in this study is therefore not the absence of 3D flood visualisation or GIS tools capable of displaying flood data, but the methodological integration of established geospatial and flood-model outputs into an end-to-end workflow that translates flood-depth rasters into consistent neighbourhood- and property-scale 3D impact information within a standard GIS environment. The individual components of the proposed approach, including terrain analysis, LiDAR-derived building representation, flood-depth rasters, and GIS-based 3D visualisation, are established techniques; the contribution lies in structuring these components into a documented GIS-native workflow that connects hydrologically and hydraulically derived flood-depth information with buildings, roads, bridges, and severity-based asset information. The study therefore focuses on the translation of existing flood information into an asset-referenced 3D communication environment rather than introducing a new hydrological, hydraulic, or rendering method.

Accordingly, the aim of this study is to develop and undertake an initial expert evaluation of a GIS-based workflow for three-dimensional visualisation of urban fluvial flood impacts. Specifically, the study seeks to: (1) integrate indicative terrain-driven hydrologic flood-depth surfaces and authoritative hydraulic flood-depth rasters within a consistent 3D GIS environment; (2) translate flood-depth information into asset-referenced outputs for buildings, roads, bridges, critical locations, and potentially safe areas; (3) examine how differences between terrain-driven and hydraulically modelled flood surfaces influence their visual representation and interpretation; and (4) assess the perceived understandability, plausibility, stability, and practical usefulness of the developed workflow through expert evaluation.

Its broader purpose, to support flood risk communication for professional and, ultimately, non-technical audiences, is assessed here only in a limited form because the present evaluation represents the first evaluation stage of the framework. The evaluation is confined to a small expert panel and is therefore treated as an initial technical and professional assessment of the framework. It does not provide

direct evidence that the 3D visualisation improves public risk perception or performs better than conventional 2D flood maps. Direct community evaluation and comparative testing with non-technical users are required as subsequent stages of research.

2. Methodology

Fig. 1 illustrates the proposed methodology, beginning with preparation of flood-depth geodatabases derived from two sources. Indicative hydrologic flood-depth rasters were generated in ArcHydro for 1 m and 2 m depth scenarios, and these were complemented by hydraulic-model output rasters supplied by Auckland Council for a 10-year flow under existing development (ED) conditions and a 100-year mean design flood scenario including climate-change effects (RCP 3.8) under maximum development probability (MPD) conditions. These depth rasters were used to delineate flood-impact areas and to assess impacts on individual buildings, bridges, and transport corridors within an urban fluvial catchment. The datasets were then translated into a 3D environment by integrating elevation rasters, LiDAR-derived building geometries, and multipatch representations, with flood depth applied consistently across terrain and assets. Flood simulation was used to represent overland flow pathways, while flood impact analysis enabled systematic classification of building and infrastructure exposure. The workflow is demonstrated for urban river flooding in a highly developed catchment, where flood behaviour is strongly influenced by terrain confinement and built infrastructure; however, its modular GIS-based design allows application to other regions, catchment scales, and flood types using equivalent depth-raster inputs.

The methodological contribution of this study does not lie in introducing a new flood model, 3D rendering technology, or standalone software platform. The underlying components, including LiDAR-derived terrain and building information, hydrologic and hydraulic flood-depth rasters, ArcGIS-based geoprocessing, and three-dimensional scene visualisation, are established techniques. Rather, the contribution lies in their structured integration within a single GIS-native workflow that translates heterogeneous flood-depth surfaces into asset-referenced 3D impact information at neighbourhood and property scales. In particular, the workflow accommodates both indicative terrain-driven hydrologic outputs and authoritative hydraulic model results within the same visualisation environment, and associates these surfaces with buildings, roads, bridges, severity information, and potentially safe areas. This provides a documented pathway from flood-model output to asset-level interpretation using standard GIS tools, rather than requiring a separately developed web, game-engine, or immersive platform.

2.1. Comparative platform assessment

A qualitative comparison of commonly used 3D and flood-visualisation platforms was undertaken to inform selection of the implementation environment (Table 1). The comparison considered accessibility, scalability, user friendliness, developer requirements, visualisation capability, and dependence on specialist hardware or external software, based on characteristics reported in the cited literature. The assessment was intended to provide contextual support for platform selection rather than a formal quantitative benchmark. Accordingly, the comparative ratings in Table 1 represent relative qualitative judgements derived from the reviewed platform characteristics and should not be interpreted as validated performance scores. They were narrowed using four key criteria of accessibility, scale identification, developer-friendliness, and user-friendliness [42–44]. Priority was given to tools that are easily obtainable and useable by a wide range of users, including community members, planners, and researchers, without requiring specialised hardware or restrictive licensing. Although the proposed workflow can be adapted for immersive virtual-reality displays (e.g. VR headsets), a desktop-based implementation was selected to ensure broad accessibility.

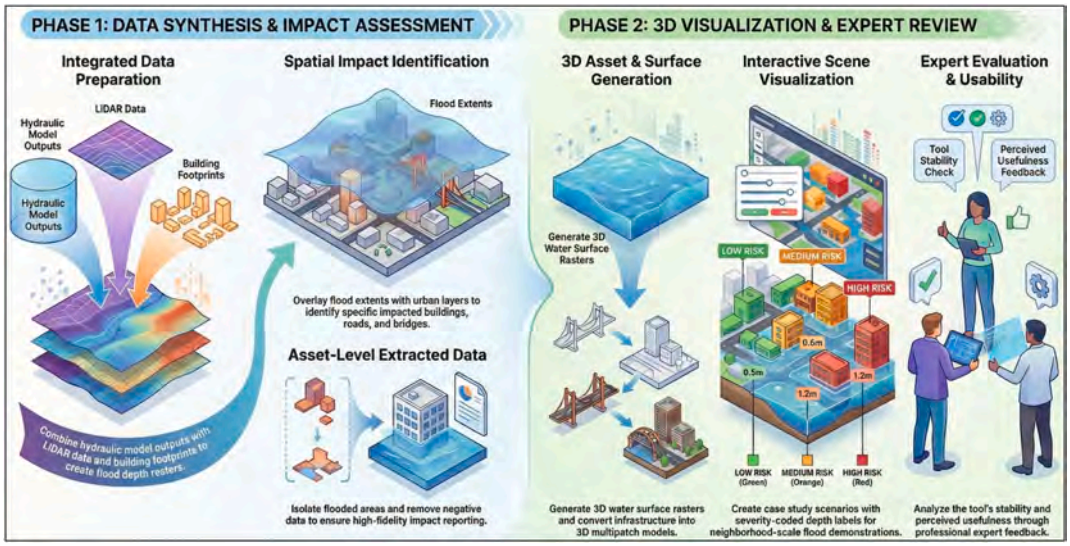


Fig. 1. Workflow of proposed 3D flood visualisation tool.

Table 1
Rapid analysis on well-explored platforms for selecting an appropriate tool.

Platform	Visualisation focus	Main function	Key implementation limitation	Accessibility/ delivery	Scalability	User interaction	Developer requirement	Reference examples
ArcGIS/ QGIS	2D/3D GIS mapping	Spatial integration, analysis and 3D visualisation	Visualisation generally depends on externally generated or separately derived hydrologic or hydraulic inputs	Desktop GIS environment	Local, catchment and broader spatial	Conventional GIS based interaction	GIS configuration and geoprocessing; limited bespoke application development	Li et al. [45]; Kuster et al. [46]
City Engine	Procedural 3D city modelling	Urban scale 3D scenario representation	Information generally requires prior GIS or external modelling preparation	Specialist 3D modelling environment	Urban and city-scale	Interactive 3D visualisation	Procedural modelling and rule configuration	Chen et al.[47]; Sermet & Demir [48]
Unity	Immersive 3D/VR	Real time interactive visualisation and custom applications	Requires external modelling and a separately developed application pipeline	Application based delivery	Dependent on application architecture and data preparation	Interactive and immersive	Game-engine application development and data integration	Dang et al. [49]; Ismael [50]
Unreal Engine	Immersive 3D/VR	High-fidelity real-time visualisation	Requires game engine workflow and, additional hardware and application development for immersive use	Application based delivery	Dependent on application and rendering configuration	Interactive and immersive	Game-engine application development and integration	Denda & Fujikane [51]; Tsujimoto et al. (2024)[52]
SketchUp	3D scene and object modelling	Construction of buildings and urban scene components	Forms part of a wider modelling or rendering workflow rather than providing simulation	Desktop 3D modelling	Local or scene-based	3D model viewing and manipulation	3D modelling and data preparation	Costabile et al. [28]
Revit/BIM	Building and asset scale representation	BIM-based flood risk and vulnerability representation	Requires integration with flood and/or GIS information for wider spatial risk assessment	Specialist BIM environment	Building and asset scale	Object and asset-based representation	BIM modelling and data management expertise	Del Duca et al. [53]
Cesium	Web based 3D	Interactive geospatial web delivery	Requires conversion and preparation of model outputs into web-compatible formats	Browser based delivery	Web-based geographic	Interactive online exploration	Web/geospatial data preparation and application configuration	Chen et al. [54]; Kumar et al. [7]
Mobile AR	Personalised, close-range 3D flood visualisation	Contextual flood risk communication	Requires development of an AR application and preparation of appropriate flood and spatial data	Low-cost AR-based delivery	Local and place-specific	Personalised interaction with flood scenarios in familiar locations	AR application development and spatial-data preparation	Gmelch et al. [55]
VR/MR headset	Immersive/mixed reality	Experiential communication and training	Requires specialist hardware and bespoke immersive application	Headset dependent	Primarily scenario and user session based	Fully immersive interaction	Bespoke application and hardware integration	Rydvanskiy & Hedley [56]

AR: Augmented reality BIM: Building Information Modelling D: Dimension MR: Mixed reality VR: Virtual reality.

Furthermore, the selected approach was required to accommodate a range of flood risk scenarios, from small catchments to national-scale analyses, ensuring flexibility for future applications. The method was also required to enable the production of robust and defensible visualisations with minimal reliance on multiple software packages, thereby streamlining the workflow from hydrological modelling to 3D visualisation. Finally, a clear and realistic visual environment was prioritised to ensure intuitive interpretation and visual clarity for non-expert users.

Thus, a GIS platform was selected due to its widespread use, well-documented capabilities for flood risk visualisation, and strong alignment with the selected evaluation criteria [5,57]. Within this environment, the flood impact analysis solution from ArcGIS Solutions was implemented, providing a structured workflow for estimating and visualising flood exposure in three dimensions.

Accordingly, ArcGIS Pro was adopted as the core implementation environment because its GIS based architecture aligned with the study requirements for integrating flood depth rasters, terrain, buildings, roads and other spatial assets within a common 3D workflow. This selection reflects the requirements of the present study rather than evidence that ArcGIS Pro is universally superior to the other reviewed platforms.

2.2. Case study demonstration

Te Auaunga (Oakley Creek) is the longest urban stream on the Auckland isthmus, located in Auckland, New Zealand, as shown in Fig. 2. The stream drains a highly urbanised catchment of approximately 12.6 km in length, flowing through residential, commercial, and transport corridors before discharging into the Waitematā Harbour [58]. Historically, Te Auaunga has experienced recurrent flooding, with documented flood events dating back to the mid-20th century [59]. Rapid urbanisation led to increased impervious surfaces, reduced infiltration, and accelerated runoff response times [60]. Early flood management strategies focused on conventional engineering solutions, including channel straightening, deepening, and concrete lining [61]. While these interventions improved conveyance locally, they also increased downstream flow velocities and did not eliminate flood risk, especially during high-intensity storms.

Flooding along Te Auaunga has continued into recent decades, with extreme rainfall events causing overtopping of the channel, inundation of adjacent properties, and damage to infrastructure. In response to these challenges, Auckland Council (AKLC) implemented a large-scale restoration and flood mitigation programme along Te Auaunga. The project combined hydraulic capacity improvements with nature-based solutions, including channel widening, re-meandering, floodplain reconnection, daylighting of piped tributaries, and wetland creation. These measures were designed to attenuate peak flows, increase temporary storage during storm events, and reduce flood risk to surrounding communities while also enhancing ecological and social values [62,63].

In terms of communication, however, AKLC flood maps mostly continued reliance on static 2D maps [62]. These flood maps are primarily developed and disseminated by regional and district councils [14]. However, the current state of these maps reveals significant limitations in their ability to effectively communicate risks, particularly to non-technical audiences. For instance, the AKLC's 2023 Flood Review highlighted how traditional methods, including 2D visualisations, contributed to delayed responses and limited situational awareness during the January 2023 Auckland floods (Auckland flood response review, 2023; Laura Robichaux, 2024; [56]).

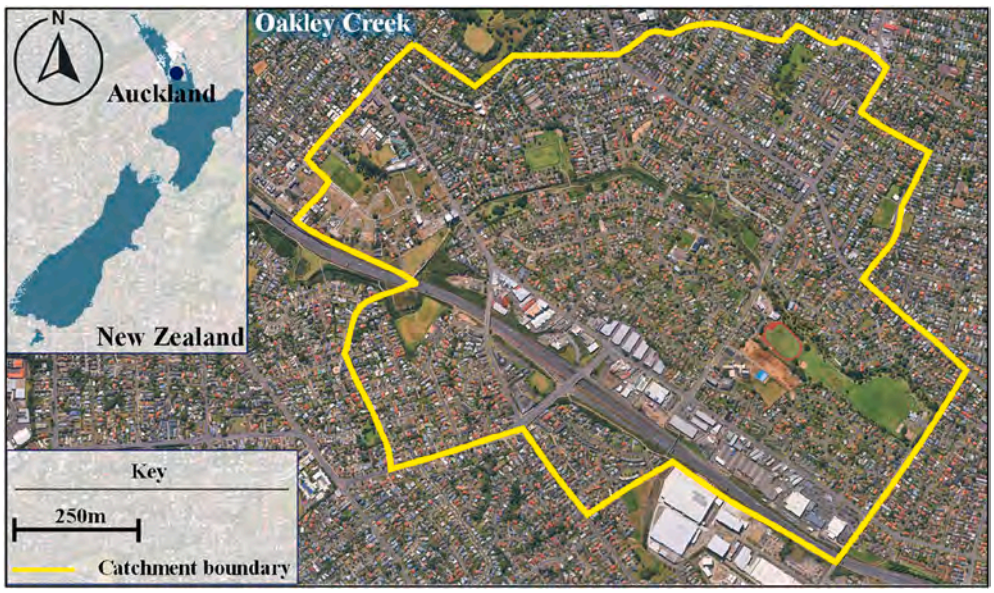


Fig. 2. Location of Te Auaunga (Oakley Creek) as case study.

2.3. Data collection and sources

The study integrates multiple geospatial and hydrological datasets, sourced primarily from AKLC and Land Information New Zealand (LINZ) to support terrain representation, urban flood modelling, and impact assessment. The DEM was used to model terrain elevation, the LiDAR point cloud provided building height information, and flood-depth rasters defined the spatial distribution and severity of inundation. A high-resolution light detection and ranging (LiDAR)-derived digital elevation model (DEM) was used as the base terrain for hydrological analysis and flood-depth mapping. To improve representation of the built environment, LiDAR point cloud data (Auckland Part 1) were employed to extract building and bridge heights and to refine 3D structural details. In addition, a 3D mesh covering the Auckland's central business district to Airport corridor (Package 2) was incorporated to provide contextual visualisation of the urban environment. Vector datasets of building outlines and road centrelines were used to characterise the built and transport infrastructure, enabling exposure and impact analyses under flood scenarios. Hydrological consistency and stream alignment were ensured through the use of the river environment classification river network within the ArcHydro framework. ArcHydro was used to generate indicative, hydrologic terrain-based flood-depth scenarios at fixed reference levels (1 m and 2 m), intended to support visual interpretation rather than represent specific design-event probabilities.

Hydraulic flood-depth raster datasets supplied by Auckland Council were used to represent event-based inundation scenarios, including a 10-year flow under ED conditions and a future 100-year flow incorporating climate-change under MPD conditions. These hydraulic scenarios were derived from council-approved modelling workflows and were incorporated into the visualisation framework without modification.

While these datasets were primarily used to develop the static flood hazard and exposure maps presented in this study, the overall framework is designed to support dynamic data integration. In particular, several of the spatial layers can be linked to relevant application programming interfaces or routinely updated data services, enabling periodic or near–real-time updates of flood extent and depth maps. This allows the mapping framework to evolve from a purely scenario-based representation toward an operational, real-time or quasi-real-time flood information system. Such integration would support timely situational awareness, facilitate rapid updates under changing hydrometeorological conditions, and enhance the applicability of the proposed approach for early warning and decision-support applications.

2.4. Applied flood scenarios

This study implemented four flood-depth scenarios to support depth-based visualisation of inundation patterns within a three-dimensional GIS environment. Two scenarios were derived using ArcHydro, which applies hydrological modelling techniques to generate terrain-based flood-depth representations from a conditioned LiDAR-derived digital elevation model. The remaining two scenarios were based on hydraulically modelled flood-depth layers provided by Auckland Council, produced through two-dimensional rainfall–runoff simulations and floodplain mapping workflows. Collectively, these scenarios enable consistent visual comparison between hydrologically derived and hydraulically modelled flood conditions.

Two flood-depth scenario types, hydrologic and hydraulic, were used to support depth-based visualisation and comparison of inundation patterns. For the ArcHydro component, fixed HAND reference stages of 1 m and 2 m were selected to illustrate contrasting

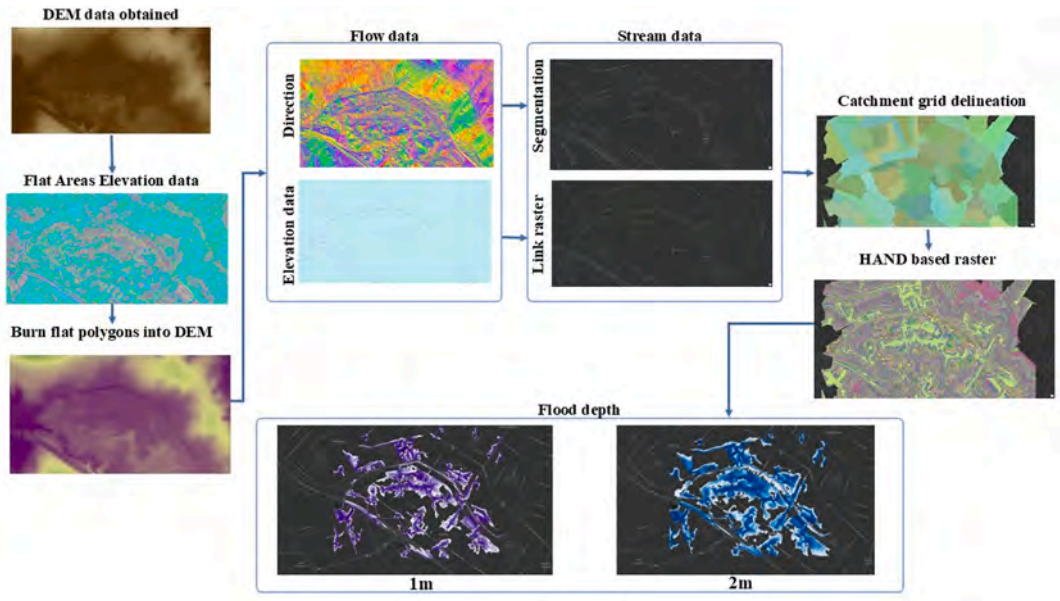


Fig. 3. ArcHydro workflow applied for generating 1 m and 2 m flood depth scenarios.

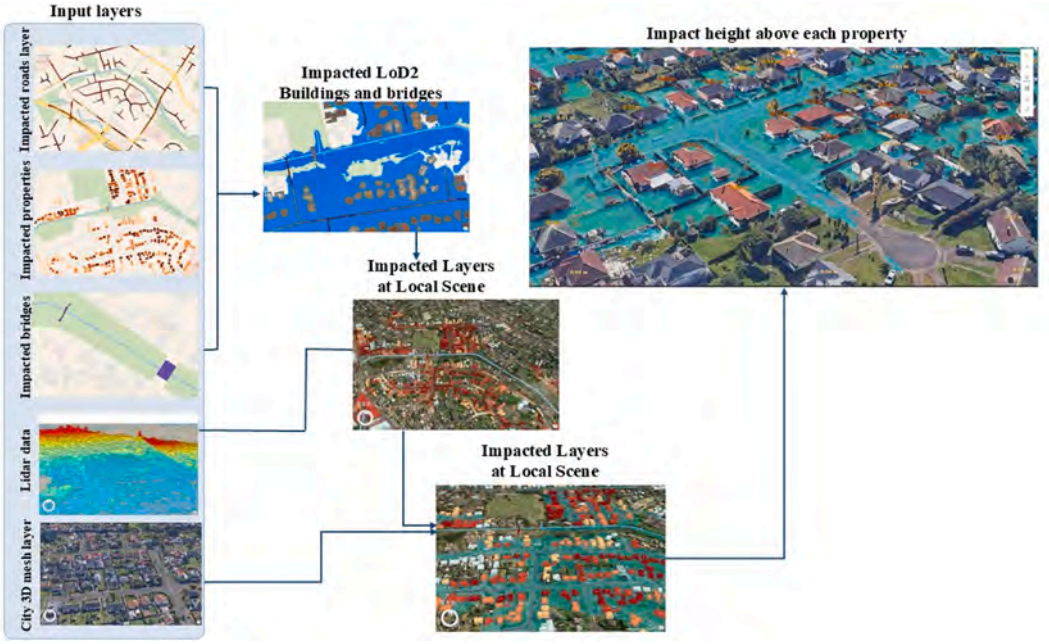


Fig. 4. 3D flood impact visualisation workflow applied through Esri's flood impact analysis solution.

lower and higher inundation conditions within the proposed visualisation framework.

The resulting 1 m and 2 m ArcHydro scenarios are therefore indicative reference scenarios used for visualisation and comparison of asset impacts, rather than calibrated representations of the 2016 event or probability-based design floods.

In addition, hydraulic flood-depth rasters produced by Auckland Council (AKLC) were incorporated to represent authoritative, scenario-based flood conditions. In Auckland practice, the 10-year Average Recurrence Interval (ARI) event is used to characterise more frequent flooding with operational and serviceability implications, while the 100-year ARI event represents a low-probability, high-impact flood and is typically adopted for floodplain mapping and planning purposes. The future 100-year scenario applied in this study incorporates climate-change allowances (+3.8 °C), reflecting projected increases in extreme rainfall intensity. These council depth rasters are derived from regionwide hydraulic modelling workflows based on two-dimensional rainfall–runoff simulations (e.g. TUFLOW), with floodplain mapping and output extraction undertaken using built-in modelling tools supported by extensive GIS automation and quality-assurance procedures [64]. The AKLC hydraulic depth rasters were visualised as provided, without alteration to the underlying modelling assumptions, and were ingested directly into the 3D visualisation workflow. This approach enabled physically modelled flood outputs to be rendered consistently within an interactive three-dimensional GIS environment. All scenarios were implemented in ArcGIS Pro 3.4 using Esri's integrated workflows.

An exploratory spatial comparison was undertaken between the ArcHydro-derived 2 m reference surface and the Auckland Council-provided TUFLOW 100-year flood-depth scenario incorporating a +3.8 °C climate-change allowance. The two rasters were harmonised to a common spatial framework for cell-based comparison. The TUFLOW raster was resampled to the ArcHydro 1 m grid using nearest-neighbour resampling, with NoData cells excluded from the comparison footprint. A minimum flood-depth threshold of 0.05 m was applied consistently to both datasets to distinguish cells included in the inundation comparison. This threshold was selected following consultation with an experienced flood-modelling practitioner. To assess sensitivity to the selected threshold, additional thresholds between 0.01 and 0.20 m were also examined. Spatial agreement was evaluated using the Jaccard similarity coefficient and directional overlap proportions between the two inundated extents. Because the ArcHydro 2 m surface is an indicative fixed-depth reference scenario rather than a probability-matched equivalent of the 100-year +3.8 °C TUFLOW hydraulic scenario, the analysis was used only to compare the spatial characteristics of the two visualisation inputs and was not treated as model validation or an accuracy assessment.

2.5. Flood depth calculation through ArcHydro

Flood-depth modelling was performed in ArcGIS Pro 3.4, employing the ArcHydro toolset to prepare terrain data, delineate catchments, and generate flood-depth rasters. This platform was selected because it integrates hydrological analysis and geo-visualisation within a single GIS environment, reducing reliance on external hydraulic software and improving accessibility for practitioners and local councils [65]. The base surface was derived from the 2025 LiDAR DEM supplied by LINZ. Pre-processing steps ensured hydrological realism: flat areas were burned into the DEM to prevent artificial stream meandering in low-gradient terrain, and bridge locations were enforced to maintain channel continuity beneath road crossings [66]. Such conditioning is essential because uncorrected DEMs can misrepresent flow paths and inflate predicted flood extents.

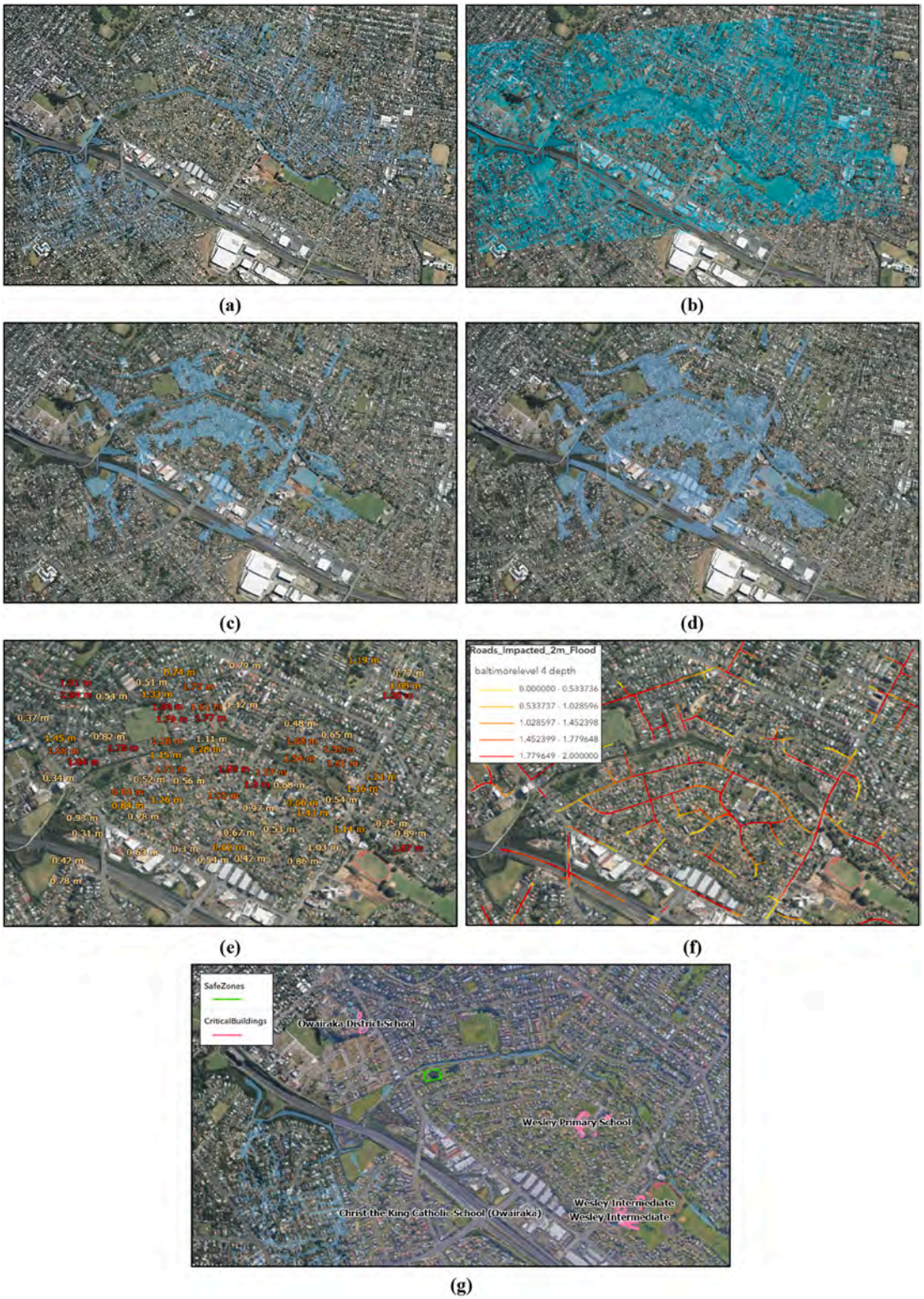


Fig. 5. Overview of the flood scenarios and asset-level outputs generated within the developed 3D GIS workflow: (a) Auckland Council 10-year hydraulic flood scenario; (b) Auckland Council 100-year hydraulic flood scenario; (c) ArcHydro-derived 1 m reference scenario; (d) ArcHydro-derived 2 m reference scenario; (e) buildings affected under the 100-year hydraulic scenario; (f) roads affected under the 100-year hydraulic scenario; and (g) identified safe areas and critical buildings under the 100-year hydraulic scenario.

From the conditioned DEM, flow-direction and flow-accumulation rasters were generated to support stream segmentation and catchment delineation. A height above nearest drainage (HAND) raster was then produced to estimate inundation extents relative to stream channels. The HAND method was chosen for its computational efficiency and clarity of output, aligning with this study's communication-focused objectives. HAND provides depth grids that are readily interpretable by stakeholders and well suited to 3D visualisation [67]. In the HAND-based approach, a 1 m scenario represents a uniform 1 m rise in water level above the channel, with all hydraulically connected areas below this elevation classified as inundated.

Two indicative depth scenarios were implemented at fixed HAND-based reference levels of 1 m and 2 m using the Define HAND-based Flood Depth and Extent tool, as illustrated in Fig. 3. Additional testing using a non-integer HAND reference stage of 1.7 m successfully generated a flood-depth raster, which was subsequently incorporated into the 3D visualisation environment. Examination of the original processing history identified an output-format configuration error, while the previously reported negative values were associated with the raster's NoData designation rather than calculated flood depths.

The selected levels provide contrasting lower- and higher-depth conditions for visualisation and asset-impact assessment and are not intended to represent specific design-event thresholds or probability-based flood events. The resulting depth rasters were incorporated into the ArcGIS Flood Impact Analysis workflow to assess building and infrastructure exposure and were subsequently visualised within a three-dimensional GIS environment.

2.6. Flood impact analysis

Flood-impact modelling was performed in ArcGIS Pro using Esri's flood impact analysis solution, which provides a structured workflow for preparing flood-depth inputs, delineating inundation extents, and visualising flood impacts in 3D (ESRI) as shown in Fig. 4. The procedure was adapted for the Oakley Creek catchment to support both indicative exposure assessment and intuitive 3D visualisation of flood scenarios derived from multiple depth-raster sources. Flood polygons were generated from both ArcHydro-derived depth rasters and authoritative hydraulic flood-depth rasters supplied by AKLC, ensuring consistency with official planning and operational flood layers. Buildings were represented using 2025 LINZ building outlines extruded into multipatch geometries based on LiDAR-derived heights. Road networks were analysed using 2016 LINZ centrelines, and bridges were mapped from manually digitised footprints with elevations refined using LiDAR point-cloud data. This overlay identified assets located within inundated areas; however, consistent with standard exposure analyses, spatial coincidence was assumed to indicate potential impact rather than direct damage.

Flood scenarios were visualised in 3D by converting depth rasters into water-surface multipatches and symbolising them relative to the underlying DEM. The incorporation of LiDAR point-cloud data enabled realistic representation of terrain and structural heights, addressing a key limitation of conventional 2D flood maps. The resulting 3D scenes are illustrative rather than predictive: depth rasters were visualised as provided, without modification to underlying hydraulics, and local flow variability and tidal-datum adjustments were not explicitly modelled.

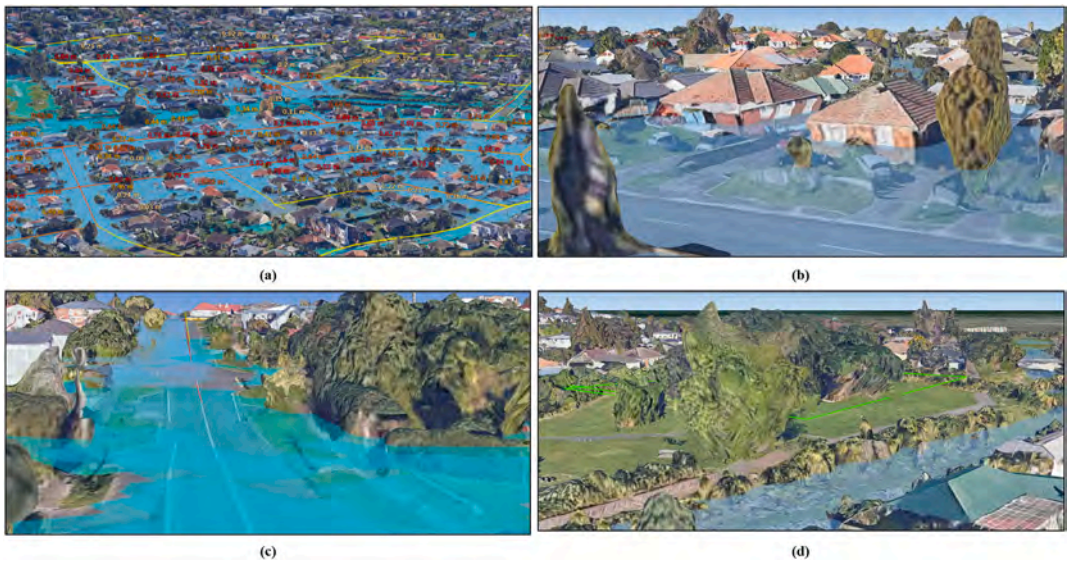


Fig. 6. 3D visualisation of the 100-year flood scenario: (a) impacted roads and buildings with severity-based criticality levels; (b) property-level representation of surface-water depth; (c) road inundation patterns and associated criticality under the simulated scenario using Auckland Council hydraulic outputs; and (d) identified safe zones and associated access routes.

2.7. Expert evaluation

The purpose of this evaluation stage was to obtain an initial professional assessment of the developed 3D flood visualisation tool prior to testing with non-technical audiences. The evaluation examined technical credibility, interpretability, operational stability, and perceived usefulness from the perspective of professionals familiar with flood risk information. It was not intended to represent public risk perception or substitute for direct community evaluation. Testing with non-technical users is therefore identified as a subsequent stage of the research.

A purposive sampling approach was adopted to target professionals with direct experience in flood risk management, spatial analysis, or flood related decision making. Invitations were sent to 15 experts working in hydrology, GIS, and flood risk management across academic, consultancy, and local government contexts. Of these, 9 experts completed the evaluation and were included in the analysis. No further narrowing or exclusion criteria were applied, and all completed responses were analysed. Participants were considered suitable based on their professional roles and experience with flood modelling, mapping, or operational flood management. The purposive expert sample was selected to provide an initial professional assessment of the framework rather than to support population level inference or evaluation of public communication effectiveness.

Prior to completing the evaluation, participants were introduced to the platform through a guided demonstration of the 3D visualisation environment. The demonstration presented multiple flood-depth scenarios rendered in the interactive 3D GIS scene, highlighting terrain representation, building-level depth labelling, road inundation, and identification of affected and safe zones which are areas that remain outside the modelled flood extent under a given scenario and are therefore not expected to experience inundation. Participants were given sufficient time to explore the visualisations and ask clarification questions before providing feedback.

The questionnaire was adapted from the expert evaluation approach used by Haynes et al. [19], who assessed expert perceptions of a flood visualisation application using structured 1 to 5 rating questions covering understandability, plausibility, stability, and usefulness. These dimensions were operationally adapted to the present 3D flood visualisation framework; the questionnaire was not treated as a formally validated psychometric instrument.

Expert feedback was collected using the adapted structured questionnaire comprising Likert-scale items designed to assess understandability, plausibility, stability, and perceived usefulness of the tool, alongside background questions relating to professional involvement, GIS experience, and familiarity with 3D modelling. Responses were recorded on a five-point Likert scale (1 = strongly disagree, 2 = disagree, 3 = neutral, 4 = agree, 5 = strongly agree). The questionnaire distinguished between four variables used to evaluate the 3D flood visualisation and three variables describing participants' professional backgrounds. The tool evaluation variables comprised understandability, plausibility, stability, and perceived usefulness. Understandability refers to the extent to which flood depth, extent, and spatial patterns could be readily interpreted from the 3D visualisation. Plausibility refers to whether the visualised flood behaviour, including depth distribution and interaction with terrain and built features, appeared credible and consistent with participants' professional knowledge and experience.

Stability refers to the perceived operational consistency of the visualisation during interaction, including smooth navigation, consistent rendering of flood surfaces, and the absence of visual or functional disruptions that could affect interpretation. Perceived usefulness refers to the potential value of the tool for practical flood risk applications, including planning, communication, and emergency management. Participant background variables comprised involvement in flood risk management, GIS experience, and 3D

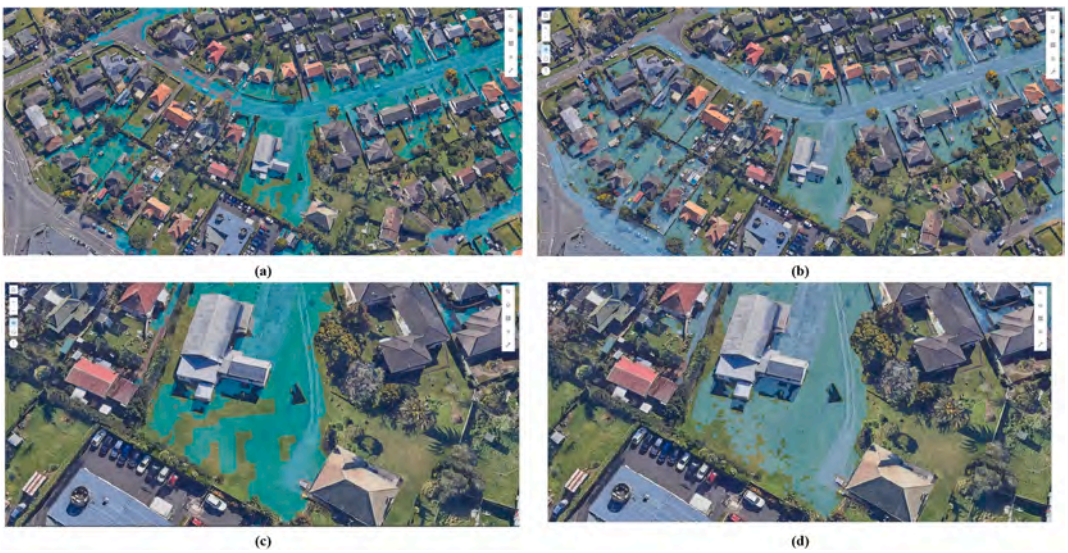


Fig. 7. Comparison of hydrological and hydraulic flood-modelling outputs: (a) Auckland Council hydraulic model output at neighbourhood scale; (b) ArcHydro-derived hydrological flood-depth visualisation at the same scale; (c) Auckland Council hydraulic model output at property scale; and (d) ArcHydro-derived hydrological flood-depth visualisation at property scale.

modelling experience. These variables were recorded separately to examine whether professional background was associated with differences in participants' assessments of the visualisation.

Responses were analysed using descriptive statistics to summarise overall trends and levels of agreement. Spearman rank correlation analysis was additionally used on an exploratory basis to examine possible associations between participants' professional backgrounds and their assessments of the visualisation. Given the small sample size, these correlation results are treated as indicative rather than confirmatory and are interpreted cautiously in the Results and Discussion. Ethical approval for this study was granted by the Massey University Human Ethics Committee, Ohu Matatika 3, following review on 24 July 2025, application reference OM3 25/42.

3. Results and discussion

From a hydroinformatic perspective, the value of the workflow lies in maintaining a structured connection between flood-depth information, terrain, and discrete urban assets within a common GIS environment. This asset-referenced structure could also provide a foundation for future digital-twin development, particularly if the workflow were extended to incorporate dynamic flood forecasts, real-time observations, regularly updated asset information, or other operational data streams. Such capabilities are not implemented in the present study, and the developed framework should therefore not be interpreted as a digital twin. Rather, the current contribution establishes a GIS-based spatial and asset-integration structure that could support more dynamic and operational applications in subsequent development.

3.1. Tool demonstration

Fig. 5 presents the 3D flood-visualisation outputs generated for the selected residential area, demonstrating how the developed approach conveys flood depth and extent within a realistic built-environment context. Fig. 5a illustrates neighbourhood-scale inundation patterns, where flood depths are overlaid directly onto terrain, buildings, and road surfaces. This representation enables rapid identification of spatial variability in flood severity, clearly distinguishing low-lying streets and local depressions with deeper inundation from elevated parcels experiencing shallower flooding.

Fig. 5b further demonstrates the applicability of the tool for communicating flood risk at a finer spatial scale, showing how individual buildings and access routes are affected under the simulated scenario. By displaying flood depths in real-world coordinates within a 3D environment, the visualisation enables flood impacts on properties and infrastructure to be examined directly in relation to the built environment.

Collectively, Fig. 5 outputs demonstrate how conventional flood-depth data can be translated into asset-referenced 3D visualisations at neighbourhood and property scales. The outputs illustrate the integration of flood depth, terrain, buildings, roads, and other spatial assets within a common GIS environment and provide a basis for subsequent professional evaluation of the developed workflow.

Fig. 6 illustrates how the developed 3D platform supports interpretation of flood impacts at the individual asset and user level under the 100-year flood scenario. The visualisation shown in Fig. 6a demonstrates how roads and buildings can be assessed simultaneously according to their flood exposure and level of criticality, allowing decision-makers to visually distinguish assets that are likely to experience greater functional disruption during flood events. This representation provides an immediate understanding of where intervention, protection, or response efforts may be most urgently required.

At the property scale, Fig. 6b highlights how surface-water depths interact with individual buildings, enabling flood impacts to be interpreted from the perspective of affected residents and property owners. By presenting flood depth directly within a three-dimensional built environment, the visualisation enables potential impacts to be examined in relation to individual buildings and surrounding spatial features. Fig. 6c focuses on surface-flooding conditions along transport corridors under the Auckland Council 100-year scenario, illustrating how inundation severity varies across the road network. This view is particularly relevant for transport planners and emergency services, as it allows potential access constraints and vulnerable road sections to be identified visually, supporting operational planning and emergency response decisions. In contrast, Fig. 6d demonstrates the identification of safe zones and their accessible routes within the flooded landscape, integrating flood extent with evacuation considerations. This capability supports both authorities and community members in understanding where safe areas are located and how they may be reached during flood events.

Taken together, the demonstrations in Fig. 6 show how the workflow translates conventional flood-model outputs into asset-referenced 3D information. The visualisations associate flood depth with buildings, roads, access routes, and identified safe areas,

Table 2
Descriptive statistics of expert responses to the developed 3D flood visualisation tool.

Variable	Mean	SD	Min	Q1	Median	Q3	Max	IQR	Skewness
Involvement	4.22	0.97	3	3	5	5	5	2	−0.55
GIS experience	3.67	0.71	3	3	4	4	5	1	0.61
3D experience	2.78	1.09	1	2	3	4	4	2	−0.19
Understandability	4.56	0.53	4	4	5	5	5	1	−0.27
Plausibility	4.22	0.44	4	4	4	4	5	0	1.62
Stability	4.56	0.53	4	4	5	5	5	1	−0.27
Usefulness	4.11	0.60	3	4	4	4	5	0	0.02

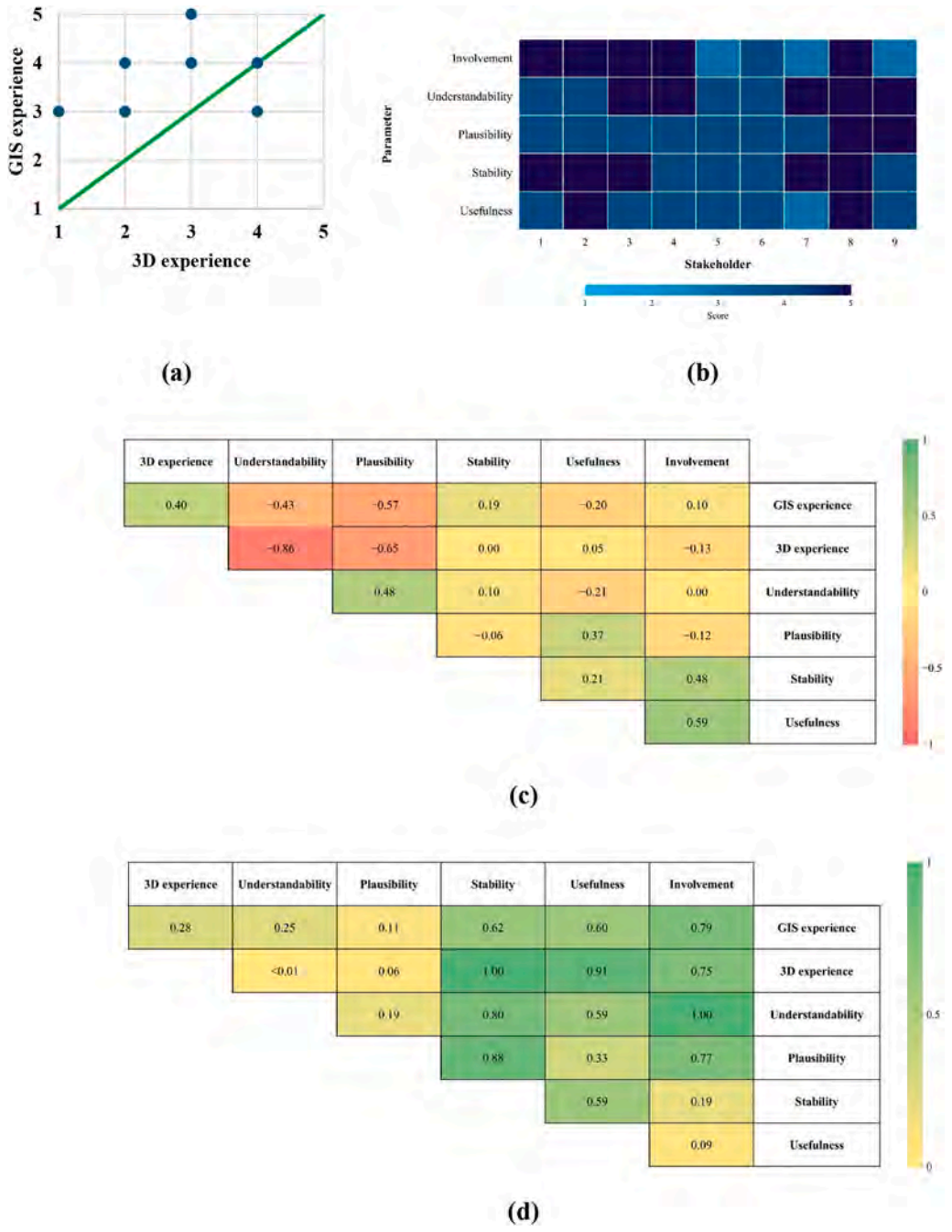


Fig. 8. Expert evaluation results: (a) relationship between GIS and 3D experience, (b) heat map of expert ratings, (c) Spearman rank correlations among participant background and tool evaluation variables, and (d) corresponding p values.

illustrating how model outputs can be examined at neighbourhood and property scales within a common GIS environment.

A qualitative comparison between the ArcHydro-derived 1 m flood scenario and the 100-year + 3.8 °C scenario depth rasters shows consistent differences in spatial pattern, depth expression, and visual structure. As Fig. 7 illustrates, the ArcHydro scenario exhibits smoother and more laterally continuous inundation patterns that broadly follow topographic lows, road corridors, and valley morphology, with gradual depth transitions across adjacent parcels. In contrast, the hydraulic depth rasters display sharper flood boundaries and greater spatial heterogeneity, with inundation more strongly constrained to the channel network and hydraulically connected overland flow paths.

An exploratory quantitative spatial comparison was also undertaken between the ArcHydro-derived 2 m reference surface and the Auckland Council-provided 100-year TUFLOW hydraulic depth raster after harmonising the datasets to a common spatial framework.

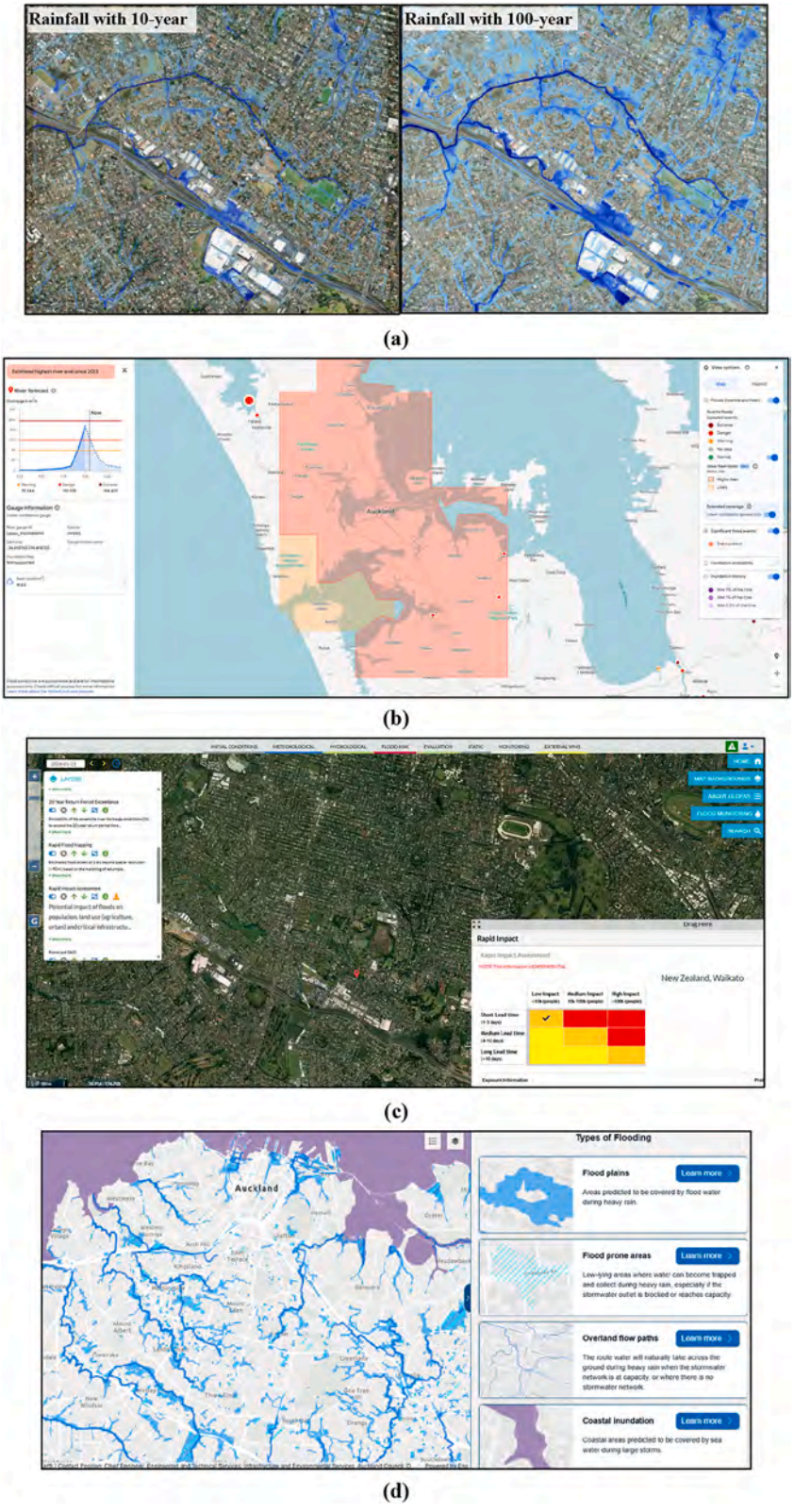


Fig. 9. Examples of selected flood-information and visualisation systems used for contextual comparison: (a) FASTFLOOD [75], (b) Google Flood Hub [76], (c) Copernicus GloFAS [77], and (d) Auckland Flood Viewer (Auckland Council, 2023).

The TUFLOW raster was resampled to the ArcHydro 1 m grid using nearest-neighbour resampling, and NoData cells were excluded from the comparison footprint. Using a minimum depth threshold of 0.05 m for the spatial comparison, the inundated extents produced a Jaccard similarity coefficient of 0.22. Approximately 98.2% of TUFLOW cells exceeding the selected threshold were also included within the corresponding ArcHydro extent, whereas 21.9% of ArcHydro cells exceeding the threshold coincided with TUFLOW cells exceeding the same threshold.

Within cells exceeding the threshold in both datasets, the mean depth was 1.23 m for the ArcHydro reference surface and 0.43 m for the TUFLOW hydraulic raster. Sensitivity checks using thresholds between 0.01 and 0.20 m produced the same overall pattern of limited spatial agreement. These statistics are interpreted only as a comparison of the spatial characteristics of the two visualisation inputs, rather than as a model validation or accuracy assessment, because the fixed 2 m ArcHydro reference surface is not a probability-matched equivalent of the 100-year TUFLOW hydraulic scenario.

Depth distributions in the hydraulic scenarios show more pronounced localised maxima, particularly within channels, road depressions, and backwater areas, whereas the ArcHydro-derived depths vary more uniformly across the floodplain. From a visualisation standpoint, the ArcHydro output provides a smoother and more generalised representation of terrain-related inundation potential, whereas the hydraulic scenarios retain greater local variation associated with channel connectivity, flow routing, and local hydraulic controls. These differences affect how the outputs should be interpreted: the ArcHydro scenarios are useful as indicative reference surfaces for examining broad spatial patterns and asset exposure, while the hydraulic outputs provide a more spatially differentiated representation of modelled flood depth. The comparison therefore illustrates complementary visualisation roles rather than evidence that one modelling approach is universally preferable.

The limited spatial agreement between the two flood-depth representations has important implications for flood-risk communication. The broader inundation extent produced by the ArcHydro reference surface may lead to different interpretations of property and infrastructure exposure compared with the hydraulic scenario, particularly regarding which buildings and roads appear inundated and the severity of flooding at individual locations. These differences become especially relevant when flood information is presented through realistic 3D visualisations, where detailed representations of terrain and buildings may create an impression of spatial precision that is not necessarily supported by the underlying flood data. Importantly, the ArcHydro 2 m reference surface and the TUFLOW 100-year climate-change scenario are not probability-matched representations of the same flood event. Their limited spatial agreement therefore should not be interpreted as evidence of relative model accuracy. Instead, the findings highlight the importance of clearly communicating modelling assumptions, scenario characteristics, and limitations when presenting property-level flood exposure through 3D visualisations.

3.2. Expert opinion evaluation

Descriptive statistics of expert responses (Table 2) reveal generally positive evaluations of the developed 3D flood-visualisation tool. Most participants indicated a moderate to high level of involvement in flood risk management (mean = 4.22) and GIS experience (mean = 3.67), while fewer had strong backgrounds in 3D modelling (mean = 2.78). Ratings of the four tool-evaluation variables were generally favourable. The visualisation was considered both "easy to understand and stable" (means = 4.56 for both), showing minimal dispersion, with a low standard deviation ($\sigma = 0.53$), indicating consistent agreement among respondents. Plausibility had a mean score of 4.22 with low dispersion (SD = 0.44), while the median and interquartile range were 4 and 0, respectively, indicating closely clustered responses within the expert sample. The perceived usefulness of the application also scored highly (mean = 4.11), indicating that the expert participants considered the visualisation potentially useful for practical flood risk applications. Given the small expert sample and ordinal nature of the Likert-scale responses, median, interquartile range, and observed minimum–maximum values are reported alongside the mean and standard deviation to provide complementary measures of central tendency and dispersion.

Fig. 8 illustrates the distribution of expert responses across the evaluation and participant background variables. Participants reported greater experience with GIS than with 3D visualisation, with median scores of 4 and 3, respectively. Fig. 8b also shows relatively high scores for involvement in flood risk management, understandability, and plausibility. The limited dispersion in the tool evaluation ratings indicates a relatively consistent pattern of responses within this expert sample.

The relationship between participant background variables and tool evaluation ratings was explored using the correlation analysis shown in Fig. 8c. The observed associations varied across the evaluated variables, with some differences evident in relation to participants' GIS and 3D modelling experience. Given the small expert sample, these patterns are treated as exploratory and are not interpreted as demonstrating systematic differences between user groups. Spearman's rank correlation analysis was used on an exploratory basis to examine associations between participants' technical backgrounds and their assessments of the visualisation, with the results presented in Fig. 8c and d. Given the small sample size, the observed correlations are interpreted as exploratory patterns rather than confirmatory relationships. A moderate positive association was observed between involvement in flood risk management and perceived usefulness ($\rho = 0.59$, $p = 0.09$). Given the exploratory nature of the analysis, this association is reported descriptively and is not interpreted as evidence of a systematic relationship. A weaker positive association was also observed between involvement in flood risk management and stability ($\rho = 0.48$, $p = 0.19$), although this pattern is likewise interpreted cautiously given the small sample.

A strong negative association was observed between 3D experience and understandability ($\rho = -0.86$, $p < 0.01$), together with a moderate negative association between 3D experience and plausibility ($\rho = -0.65$, $p = 0.06$). This exploratory pattern may indicate

that participants with greater 3D modelling experience evaluated the visualisation more critically. Given the small sample size, however, the observed association should not be interpreted as evidence of a systematic effect of prior experience or as evidence of performance among non-technical users.

The expert evaluation produced generally favourable ratings for understandability, plausibility, stability, and perceived usefulness. These findings provide preliminary professional feedback on the developed visualisation framework, while the small purposive sample and absence of direct testing with non-technical users limit broader conclusions regarding communication effectiveness.

3.3. Applicability of the developed tool

To place the developed workflow within the wider flood-visualisation landscape, a descriptive comparison was made with four existing flood-information and visualisation systems: FASTFLOOD (Coulthard, 2013; [68–70]), Google Flood Hub [71], Copernicus Global Flood Emergency Viewer [72,73], and the Auckland Flood Viewer [14,74]. These examples represent different approaches to communicating flood information across global, regional, and local contexts. The comparison is intended only to contextualise differences in visual presentation, spatial scale, and information delivery; it is not a formal benchmark of modelling accuracy, platform performance, usability, or communication effectiveness.

Fig. 9 illustrates representative outputs from the selected systems. Their interfaces primarily communicate flood information through map-based representations of variables such as inundation extent, depth, return-period information, or other flood-hazard indicators, depending on the purpose and underlying data of each system. These systems operate at different spatial scales and serve different operational or informational purposes, and no direct equivalence between their modelling approaches and the workflow developed in this study is assumed.

The comparison highlights a distinction in visualisation scale and representation rather than relative platform performance. The selected external systems predominantly provide map-based flood information across relatively broad spatial extents, whereas the workflow developed in this study links flood-depth surfaces directly with individual buildings, roads, bridges, access routes, and other urban assets within a 3D GIS environment. This enables flood information to be examined at neighbourhood and property scales while retaining the spatial relationship between the flood surface and discrete assets.

The developed workflow should therefore be viewed as complementary to, rather than a replacement for, established flood-information systems. Its particular role is the asset-referenced 3D representation of existing flood-model outputs within a GIS environment. Whether this form of representation improves understanding, usability, or decision-making relative to other platforms would require direct comparative evaluation and is not established by the present study.

In practical terms, the workflow may support different professional tasks by linking flood depth directly to discrete urban assets within a familiar GIS environment. For flood managers and planners, this can assist spatial inspection of affected buildings, roads, and neighbourhood-scale exposure. For emergency responders, the representation of inundated roads, potentially affected access routes, and identified safe areas provides a spatial basis for examining operational constraints. For community-facing applications, the asset-referenced 3D outputs provide a format that could be used in future engagement or communication activities, although effectiveness for non-technical users was not evaluated in the present study. Compared with visualisation frameworks that rely primarily on standalone web interfaces, game engines, immersive environments, or broad-scale map viewers, the present workflow contributes a GIS-native pathway that retains flood-model outputs, terrain, and managed urban assets within the same spatial environment.

4. Conclusion

This study presented a GIS-based workflow for producing three-dimensional flood visualisations aimed at improving flood risk communication in urban fluvial settings. Using Te Auaunga (Oakley Creek) as a case study, the work demonstrated how both indicative, terrain-based flood-depth surfaces and council-approved hydraulic flood-depth rasters can be integrated and visualised within a standard GIS environment. The proposed approach enables commonly available flood-model outputs to be presented in a spatial form that supports interpretation at neighbourhood and property scales, without reliance on bespoke visualisation platforms or specialised hardware.

The developed visualisations represent flood depth in relation to terrain, buildings, and transport infrastructure, enabling inundation patterns and asset exposure to be examined within their spatial context. The inclusion of building-level depth information, road inundation, and areas outside the modelled flood extent enables flood exposure to be examined in relation to individual properties and surrounding infrastructure.

Findings from the expert evaluation indicate that the developed visualisations were generally regarded as understandable, stable, and plausible. Participants with operational flood risk management experience reported higher perceived usefulness, while those with stronger backgrounds in 3D modelling tended to apply more critical judgement to visual simplifications. This variation reflects differences in professional expectations and indicates that perceptions of the visualisation may be influenced by participants' professional backgrounds and prior experience. These findings represent exploratory, perception-based assessments from a small group of professionals and should not be interpreted as evidence of improved flood-risk comprehension or communication effectiveness among non-technical audiences.

The comparative assessment demonstrates that the proposed workflow complements existing flood-information platforms. Regional and global systems remain essential for providing consistent, authoritative flood intelligence at broad spatial scales, whereas the GIS-based 3D approach developed here supports more detailed, asset-focused interpretation using existing flood-depth datasets. The comparison between terrain-based and hydraulically modelled flood-depth surfaces highlights that each representation conveys

different but complementary information. The ArcHydro-derived surfaces produced smoother and more laterally continuous inundation patterns, whereas the hydraulically modelled rasters exhibited sharper flood boundaries and greater localised depth variability associated with flow routing and hydraulic controls. In this way, the workflow addresses a specific gap between technical flood modelling outputs and local-scale understanding required for planning, preparedness, and stakeholder engagement. Further work should focus on improving temporal alignment between terrain and urban representation datasets, incorporating additional hydraulically derived variables where available, and extending evaluation to include community participants. As the workflow is modular and data-driven, such refinements can be implemented without changes to the underlying methodology.

A further limitation concerns the exploratory comparison between the ArcHydro-derived 2 m reference surface and the Auckland Council-provided TUFLOW 100-year +3.8 °C climate-change hydraulic depth raster. These two surfaces are not probability-matched representations of the same flood event; the ArcHydro layer is an indicative fixed-depth reference scenario, whereas the TUFLOW raster represents a specific hydraulic design scenario. Accordingly, the reported spatial-overlap statistics should be interpreted as a comparison of visualisation inputs rather than as model validation or an assessment of relative accuracy. The 0.05 m inundation threshold used for the comparison was selected following expert consultation and, although sensitivity checks across thresholds from 0.01 to 0.20 m produced the same general pattern, the resulting overlap measures remain dependent on the adopted comparison framework.

The present study did not include a direct experimental comparison between the developed 3D visualisation and conventional 2D flood maps. Comparative evaluation of map-based flood risk communication has been recognised as an important methodological consideration in previous research, and future work should therefore include controlled 2D-versus-3D testing with non-technical users to determine whether the 3D representation provides measurable communication benefits.

Overall, the study demonstrates a practical GIS-native pathway for integrating flood-depth information with terrain, buildings, roads, and other spatial assets in an interactive 3D environment. Future work could extend the proposed framework by connecting the 3D visualisations to relevant application programming interfaces supplying updated flood, rainfall, or hydrological information. This would enable dynamic updating of flood-depth layers within the GIS environment, allowing the visualisations to evolve from static scenario representations toward near–real-time or event-responsive flood-information tools, while remaining grounded in established modelling workflows.

CRediT authorship contribution statement

Fatemeh Kaleshani: Writing – original draft, Visualization, Methodology, Investigation, Data curation, Conceptualization. **Mostafa Babaeian Jelodar:** Writing – review & editing, Supervision, Methodology, Conceptualization. **Farzad Piadeh:** Writing – review & editing, Supervision, Methodology, Conceptualization. **Suzanne Wilkinson:** Writing – review & editing, Supervision. **Bruce Balaei:** Writing – review & editing, Supervision.

Declaration of competing interest

The authors declare that they have no known competing financial interests or personal relationships that could have appeared to influence the work reported in this paper.

Appendix A. Supplementary data

Supplementary data to this article can be found online at https://doi.org/10.1016/j.ijdrr.2026.106548.

Data availability

I have shared my data as supplementary document.

References

[1] C.D. Girotto, F. Piadeh, V. Bakhtiari, K. Behzadian, A.S. Chen, L.C. Campos, M. Zolgharni, A critical review of digital technology innovations for early warning of water-related disease outbreaks associated with climatic hazards, Int. J. Disaster Risk Reduct. 100 (2024), https://doi.org/10.1016/j.ijdrr.2023.104151.
[2] F. Piadeh, V. Bakhtiari, F. Piadeh, Automated novel real-time framework for rainfall data imputation in flood early warning systems, Eng. Appl. Artif. Intell. 164 (2026), https://doi.org/10.1016/j.engappai.2025.113348.
[3] R. De Santis, F. Macchione, P. Costabile, C. Costanzo, N. Rivière, A comparative analysis of 3-D representations of urban flood map in virtual environments for hazard communication purposes, E3S Web of Conferences 40 (2018), https://doi.org/10.1051/e3sconf/20184006037.
[4] F. Macchione, P. Costabile, C. Costanzo, R. De Santis, Moving to 3-D flood hazard maps for enhancing risk communication, Environ. Model. Software 111 (2019) 510–522, https://doi.org/10.1016/j.envsoft.2018.11.005.
[5] V. Bakhtiari, F. Piadeh, A.S. Chen, K. Behzadian, Stakeholder analysis in the application of cutting-edge digital visualisation technologies for urban flood risk management: a critical review, Expert Syst. Appl. 236 (2024), https://doi.org/10.1016/j.eswa.2023.121426.
[6] K.E. McNamara, R. Clissold, R. Westoby, A.E. Piggott-McKellar, R. Kumar, T. Clarke, F. Namoumou, F. Areki, E. Joseph, O. Warrick, P.D. Nunn, An assessment of community-based adaptation initiatives in the Pacific Islands, Nat. Clim. Change 10 (7) (2020) 628–639, https://doi.org/10.1038/s41558-020-0813-1.
[7] V. Kumar, K. Sharma, T. Caloiero, D. Mehta, K. Singh, Comprehensive overview of flood modeling approaches: a review of recent advances, Hydrology 10 (7) (2023), https://doi.org/10.3390/hydrology10070141.

[8] V. Jean, M.-A. Boucher, A. Frini, D. Roussel, Uncertainty in three dimensions: the challenges of communicating probabilistic flood forecast maps, Hydrol. Earth Syst. Sci. 27 (18) (2023) 3351–3373, https://doi.org/10.5194/hess-27-3351-2023.
[9] Y. Li, Z. Gao, D. Wang, J. Sun, G. Zhang, J. Gong, Multilevel data simplification methods for flood process visualizations based on visual perceptions, Int. J. Digit. Earth 17 (1) (2024), https://doi.org/10.1080/17538947.2024.2323180.
[10] R. Naghedi, X. Huang, F. Piadeh, K. Behzadian, Flood impacts on transportation infrastructure: critical review on current trends and future perspectives, Nat. Hazards Rev. 27 (3) (2026), https://doi.org/10.1061/NHREFO.NHENG-255.
[11] J.S. Lai, W.-Y. Chang, Y.-C. Chan, S.-C. Kang, Y.-C. Tan, Development of a 3D virtual environment for improving public participation: case study – the Yuansantze Flood Diversion Works Project, Adv. Eng. Inform. 25 (2) (2011) 208–223, https://doi.org/10.1016/j.aei.2010.05.008.
[12] W. Li, J. Zhu, J.-H. Haunert, L. Fu, Q. Zhu, Y. Dehbi, Three-dimensional virtual representation for the whole process of dam-break floods from a geospatial storytelling perspective, Int. J. Digit. Earth 15 (1) (2022) 1637–1656, https://doi.org/10.1080/17538947.2022.2118877.
[13] J. Zhu, J. Wu, Y. Guo, J. Zhang, Z. Guo, P. Dang, W. Li, Multi-level enhanced visualization of virtual geographic scenes for improving risk perception: a case study of flood disaster scenes, Environ. Model. Software 196 (2026) 106757, https://doi.org/10.1016/j.envsoft.2025.106757.
[14] W. Auliagisni, S. Wilkinson, M. Elkharboutly, Using community-based flood maps to explain flood hazards in Northland, New Zealand, Prog. Disaster Sci. 14 (2022) 100229, https://doi.org/10.1016/j.pdisas.2022.100229.
[15] Q. Ma, B. Millet, Design guidelines for hurricane risk forecast to non-expert users, Proc. Hum. Factors Ergon. Soc. Annu. Meet. 66 (1) (2022) 2031–2035, https://doi.org/10.1177/1071181322661158.
[16] F. Piadeh, K. Behzadian, A. Chen, Z. Kapelan, J. Rizzuto, L. Campos, Enhancing urban flood forecasting in drainage systems using dynamic ensemble-based data mining, Water Res. 247 (2023) 120791, https://doi.org/10.1016/j.watres.2023.120791.
[17] S. Amirebrahimi, A. Rajabifard, P. Mendis, T. Ngo, A BIM-GIS integration method in support of the assessment and 3D visualisation of flood damage to a building, Journal of Spatial Science 61 (2) (2016) 317–350, https://doi.org/10.1080/14498596.2016.1189365.
[18] H. Singh, R.D. Garg, Web 3D GIS application for flood simulation and querying through open source technology, J. Indian Soc. Remote Sens. 44 (4) (2016) 485–494, https://doi.org/10.1007/s12524-015-0498-5.
[19] P. Haynes, S. Hehl-Lange, E. Lange, Mobile augmented reality for flood visualisation, Environ. Model. Software 109 (2018) 380–389, https://doi.org/10.1016/j.envsoft.2018.05.012.
[20] A. D'Amico, G. Bernardini, R. Lovreglio, E. Quagliarini, A non-immersive virtual reality serious game application for flood safety training, Int. J. Disaster Risk Reduct. 96 (2023), https://doi.org/10.1016/j.ijdrr.2023.103940.
[21] M. Mirza, A. Clark, S. Lukosch, H. Lukosch, Risk perception and awareness in an augmented reality flood response game: the role of player perspectives, Computers in Human Behavior Reports 18 (2025), https://doi.org/10.1016/j.chbr.2025.100657.
[22] Z. Zhang, Q. Li, Q. Sun, L. Ceferino, Using virtual reality to study human response to flood risk across controlled experiments, Int. J. Disaster Risk Reduct. 132 (2026), https://doi.org/10.1016/j.ijdrr.2025.105956.
[23] R. Tsujimoto, T. Fukuda, N. Yabuki, Server-enabled mixed reality for flood risk communication: On-site visualization with digital twins and multi-client support, Environ. Model. Software 177 (2024) 106054, https://doi.org/10.1016/j.envsoft.2024.106054.
[24] S. Kaynak, B. Kaynak, O. Mermer, I. Demir, City-scale digital twin framework for flood impact analysis: integrating urban infrastructure and real-time data analytics, Urban Clim. 64 (2025) 102640, https://doi.org/10.1016/j.uclim.2025.102640.
[25] C. Fan, J. Hou, X. Li, G. Song, Y. Yang, X. Liang, Q. Zhou, M. Imran, G. Chen, Z. Wang, P. Lu, Efficient urban flood control and drainage management framework based on digital twin technology and optimization scheduling algorithm, Water Res. 282 (2025) 123711, https://doi.org/10.1016/j.watres.2025.123711.
[26] X. Wang, H. Shu, Y. Liu, J. Guo, Z. Jiang, Y. Xu, L. Song, Y. Cao, High speed flash flood deduction and prevention method based on three-dimensional digital twin scene, J. Hydrol.: Reg. Stud. 62 (2025), https://doi.org/10.1016/j.ejrh.2025.102825.
[27] R. Sajja, O. Mermer, Y. Sermet, I. Demir, Hydro3DJS: a modular web-based library for real-time 3D visualization of watershed dynamics and digital twin integration, Environ. Model. Software 197 (2026) 106853, https://doi.org/10.1016/j.envsoft.2025.106853.
[28] P. Costabile, C. Costanzo, G. De Lorenzo, R. De Santis, N. Penna, F. Macchione, Terrestrial and airborne laser scanning and 2-D modelling for 3-D flood hazard maps in urban areas: new opportunities and perspectives, Environ. Model. Software 135 (2021) 104889, https://doi.org/10.1016/j.envsoft.2020.104889.
[29] R.J. Meyer, J. Baker, K. Broad, J. Czajkowski, B. Orlove, The dynamics of hurricane risk perception: real-time evidence from the 2012 Atlantic hurricane season, Bull. Am. Meteorol. Soc. 95 (9) (2014) 1389–1404, https://doi.org/10.1175/bams-d-12-00218.1.
[30] S. Schneiderbauer, P. Fontanella Pisa, J.L. Delves, L. Pedoth, S. Rufat, M. Erschbamer, T. Thaler, F. Carnelli, S. Granados-Chahin, Risk perception of climate change and natural hazards in global mountain regions: a critical review, Sci. Total Environ. 784 (2021) 146957, https://doi.org/10.1016/j.scitotenv.2021.146957.
[31] G. Banerski, K. Abramczuk, Persuasion illustrated: motivating people to undertake self-protective measures in case of floods using 3D animation focused on components of protection motivation theory, Int. J. Disaster Risk Reduct. 89 (2023) 103575, https://doi.org/10.1016/j.ijdrr.2023.103575.
[32] O.V. Wilhelmi, R.E. Morss, H. Lazrus, J. Boehnert, J.M. Gambill, Examining the roles of visualizations in people's understanding of uncertain storm surge forecasts, interpretation of risk, and decision-making, Int. J. Disaster Risk Reduct. 107 (2024), https://doi.org/10.1016/j.ijdrr.2024.104424.
[33] K.R. Saunders, O. Forbes, J.K. Hopf, C.R. Patterson, S.A. Vollert, K. Brown, R. Browning, M.A. Canizares, R.S. Cottrell, L. Li, C.J.S. Kim, T.P. Stewart, C. Susilawati, X.Y. Zhao, K.J. Helmstedt, Data-driven recommendations for enhancing real-time natural hazard warnings, One Earth 8 (5) (2025) 101274, https://doi.org/10.1016/j.oneear.2025.101274.
[34] M. Afra, M. Nazari, M.H. Kayhani, M. Sharifpur, J.P. Meyer, 3D experimental visualization of water flooding in proton exchange membrane fuel cells, Energy 175 (2019) 967–977, https://doi.org/10.1016/j.energy.2019.03.128.
[35] G. Zhi, Z. Liao, W. Tian, J. Wu, Urban flood risk assessment and analysis with a 3D visualization method coupling the PP-PSO algorithm and building data, J. Environ. Manag. 268 (2020) 110521, https://doi.org/10.1016/j.jenvman.2020.110521.
[36] Y.-C. Chiang, T.-Y. Ling, Exploring flood resilience thinking in the retail sector under climate change: a case study of an estuarine region of Taipei City, Sustainability 9 (9) (2017), https://doi.org/10.3390/su9091650.
[37] M. Simpson, L. Padilla, K. Keller, A. Klippel, Immersive storm surge flooding: scale and risk perception in virtual reality, J. Environ. Psychol. 80 (2022) 101764, https://doi.org/10.1016/j.jenvp.2022.101764.
[38] J. Blay, M. Fawakherji, L. Hashemi-Beni, Flood Impact Risk Mapping in Settlement Areas from a 3D Perspective: a Case Study of Hurricane Matthew, IGARSS 2024 - 2024 IEEE International Geoscience and Remote Sensing Symposium, 2024, 7-12 July 2024.
[39] O.E.J. Wing, P.D. Bates, A.M. Smith, C.C. Sampson, K.A. Johnson, J. Fargione, P. Morefield, Estimates of present and future flood risk in the conterminous United States, Environ. Res. Lett. 13 (3) (2018) 1–7, https://doi.org/10.1088/1748-9326/aaac65.
[40] L. Cea, P. Costabile, Flood risk in urban areas: modelling, management and adaptation to climate change. A review, Hydrology 9 (3) (2022) 50.
[41] G. Banerski, K. Abramczuk, C. Biele, 3D or not 3D? Evaluation of the effectiveness of 3D-enhanced warning messages for communication in crisis situations, Saf. Sci. 132 (2020), https://doi.org/10.1016/j.ssci.2020.104961.
[42] M. Martínez-Sepúlveda, J. Martí, M. López-Saavedra, VOLCANBOX: a software platform for volcanic hazard assessment, Int. J. Disaster Risk Reduct. 113 (2024), https://doi.org/10.1016/j.ijdrr.2024.104817.
[43] A. Liaskos, G.P. Petropoulos, N. Evelpidou, S.E. Detsikas, CVIc: a web platform for automated Coastal Vulnerability Index-based assessment, Environ. Model. Software 194 (2025), https://doi.org/10.1016/j.envsoft.2025.106705.
[44] D.A. Thakur, A. Sharma, M.P. Mohanty, Development of multi-hazard flood risk information system for coastal region: a consolidated end-to-end web platform for efficient flood management, Environ. Sustain. Indic. 29 (2026), https://doi.org/10.1016/j.indic.2026.101115.
[45] S. Li, M. Goldberg, S. Kalluri, D.T. Lindsey, B. Sjoberg, L. Zhou, S. Helfrich, D. Green, D. Borges, T. Yang, D. Sun, High resolution 3D mapping of hurricane flooding from moderate-resolution operational satellites, Remote Sens. 14 (21) (2022), https://doi.org/10.3390/rs14215445.
[46] F. Kuster, I.T. Ruginski, S.I. Fabrikant, How does your viewing perspective matter for decision-making with flood risk maps? Cartogr. Geogr. Inf. Sci. 50 (6) (2023) 562–573, https://doi.org/10.1080/15230406.2023.2268502.

[47] A.S. Chen, M. Khoury, L. Vamvakeridou-Lyroudia, D. Stewart, M. Wood, D.A. Savic, S. Djordjevic, 3D visualisation tool for improving the resilience to urban and coastal flooding in Torbay, UK, Procedia Eng. 212 (2018) 809–815, https://doi.org/10.1016/j.proeng.2018.01.104.
[48] Y. Sermet, I. Demir, Flood Action VR: a virtual reality framework for disaster awareness and emergency response training, in: Proceedings of the 15th International Conference on Modeling, Simulation and Visualization Methods (MSV'18), CSREA Press, 2018, pp. 65–69.
[49] P. Dang, J. Zhu, Y. Zhou, Y. Rao, J. You, J. Wu, M. Zhang, W. Li, A 3D-Panoramic fusion flood enhanced visualization method for VR, Environ. Model. Software 169 (2023), https://doi.org/10.1016/j.envsoft.2023.105810.
[50] D. Ismael, Immersive visualization in infrastructure planning: enhancing long-term resilience and sustainability, Energy Effic. 17 (7) (2024), https://doi.org/10.1007/s12053-024-10270-5.
[51] M. Denda, M. Fujikane, Development of a virtual flood experience system and its suitability as a flood risk communication tool, Proceedings of IAHS 386 (2024) 21–26, https://doi.org/10.5194/piahs-386-21-2024.
[52] J. Levy, D. Liu, Extended reality (XR) environments for flood risk management with 3D GIS and open source 3D graphics cross-platform game engines: advances in immersive sea level rise planning technologies for student learning and community engagement, in: Proceedings of 7th ASRES International Conference on Intelligent Technologies, 2023, pp. 271–285, https://doi.org/10.1007/978-981-99-1912-3_25.
[53] G. Del Duca, G. Rocha, M. Orszt, L. Mateus, A preliminary contribution towards a risk-based model for flood management planning using BIM: a case study of Lisbon, Sensors 22 (19) (2022), https://doi.org/10.3390/s22197456.
[54] Z. Chen, K. Li, J. Du, Y. Chen, R. Liu, Y. Wang, Three-dimensional simulation of regional urban waterlogging based on high-precision DEM model, Nat. Hazards 108 (3) (2021) 2653–2677, https://doi.org/10.1007/s11069-021-04793-8.
[55] P. Gmelch, R. Lejano, E. O'Keeffe, D.F. Laefer, C. Drell, M. Bertolotto, U. Ofterdinger, J. McKinley, The case for low-cost, personalized visualization for enhancing natural hazard preparedness. The international archives of the photogrammetry, remote sensing and spatial information sciences, XLIV-M-2-2020 (2020) 37–44, https://doi.org/10.5194/isprs-archives-XLIV-M-2-2020-37-2020.
[56] R. Rydvanskiy, N. Hedley, Mixed reality flood visualizations: reflections on development and usability of current systems, ISPRS Int. J. GeoInf. 10 (2) (2021), https://doi.org/10.3390/ijgi10020082.
[57] K. Kumar, H. Ledoux, J. Stoter, Dynamic 3d visualization of floods: case of the Netherlands. The international archives of the photogrammetry, remote sensing and spatial information sciences, XLII-4/W10 (2018) 83–87, https://doi.org/10.5194/isprs-archives-XLII-4-W10-83-2018.
[58] Auckland Council, Te Auaunga Awa (Oakley Creek),Long Term Strategy to 2040 and Implementation Plan 2016-2019 Auckland Council, Retrieved from, https://www.aucklandcouncil.govt.nz/content/dam/ac/docs/about-council/local-boards/puketapapa/te-auaunga-oakley-creek-vision-restoration-strategy.pdf, 2016.
[59] C.S. Richard Smedley, Nitche Nadia, A LARGE INTEGRATED STORMWATER SOLUTION FOR OAKLEY FLOODING – AUCKLAND Water New Zealand Stormwater Conference, 2013.
[60] New Zealand Institute of Landscape Architects (NZILA), Showcase Te Auaunga Oakley Creek, 2019. https://nzila.co.nz/directory/boffa-miskell-ltd-auckland.
[61] S. Woodfield, B. Wood, A Rocha Aotearoa New Zealand, Te Auaunga/Oakley Creek and Auckland flooding, A Rocha Aotearoa New Zealand (2023). https://arocha.org.nz/blog/te-auaunga-oakley-creek-and-auckland-flooding/.
[62] Auckland Council, Auckland Council Makes it Easier to Access Flood Data, Auckland Council, 2023. https://ourauckland.aucklandcouncil.govt.nz/news/2023/08/auckland-council-makes-it-easier-to-access-flood-data/.
[63] Auckland Council, R, Auckland Council Flood Viewer, Auckland Council, 2023. https://experience.arcgis.com/experience/cbde7f2134404f4d90adce5396a0a630.
[64] C. Bai, L. Zhao, AUCKLAND REGIONWIDE FLOOD MODELLING water New Zealand. https://www.waternz.org.nz/Article?Action=View&Article_id=2172, 2022.
[65] ESRI, ArcGIS solutions: archived help. https://doc.arcgis.com/en/arcgis-solutions/latest/get-started/pdf/ArcGISSolutionsArchivedHelp_ArcGISOnline.pdf, 2026.
[66] S.H. Sadeghi, M. Moradi Dashtpagerdi, H. Moradi Rekabdarkoolai, J.M. Schoorl, Sensitivity analysis of relationships between hydrograph components and landscapes metrics extracted from digital elevation models with different spatial resolutions, Ecol. Indic. 121 (2021) 107025, https://doi.org/10.1016/j.ecolind.2020.107025.
[67] H. Sabeh, C. Abdallah, N. Chahinian, M.-G. Tournoud, R. Hdeib, R. Moussa, Evaluating terrain-based HAND-SRC flood mapping model in low-relief rural plains using high resolution topography and crowdsourced data, J. Hydrol. 652 (2025) 132649, https://doi.org/10.1016/j.jhydrol.2024.132649.
[68] P. Steer, P. Davy, D. Lague, T. Bernard, H. Feliciano, Fastflood: a Fast and Simple 2D Hydrodynamic or Hydrostatic Numerical Solution to River Flow in Landscape Evolution Models, European Geosciences Union General Assembly 2022 (EGU22), Vienna, Austria, 2022, 2022-05-23, https://doi.org/10.5194/egusphere-egu22-3142.
[69] C.S. Watson, M. Creed, J. Gyawali, S. Shadeed, J. Dabbeek, D.L. Subedi, R. Haiju, Earth observation informed modelling of flash floods, Int. J. Disaster Risk Reduct. 132 (2026) 105977, https://doi.org/10.1016/j.ijdrr.2025.105977.
[70] J. Tom, J.C.N. Coulthard, Paul D. Bates, Jorge Ramirez, Gustavo A.M. de Almeida, Greg R. Hancock, Integrating the LISFLOOD-FP 2D Hydrodynamic Model with the CAESAR Model: Implications for Modelling Landscape Evolution, WILEY, 2013, https://doi.org/10.1002/esp.3478.
[71] E. Kuipers, V. Oldenburg, E. Sutanudjaja, P. Phung, A. Ficchì, M. van den Homberg, Assessing the riverine flood forecast skill of GloFAS and Google Flood Hub with impact data and river flow observations to support early actions in Mali. https://doi.org/10.5194/egusphere-egu25-302, 2026.
[72] F.A. Hirpa, P. Salamon, H.E. Beck, V. Lorini, L. Alfieri, E. Zsoter, S.J. Dadson, Calibration of the Global Flood Awareness System (GloFAS) using daily streamflow data, J. Hydrol. 566 (2018) 595–606, https://doi.org/10.1016/j.jhydrol.2018.09.052.
[73] G. Matthews, C. Baugh, C. Barnard, C. Carton De Wiart, J. Colonese, S. Grimaldi, D. Ham, E. Hansford, S. Harrigan, S. Heiselberg, H. Hooker, S. Hossain, C. Mazzetti, L. Milano, F. Moschini, K. O'Regan, F. Pappenberger, D. Pfister, R.M. Rajbhandari, C. Prudhomme, Chapter 15 - on the operational implementation of the Global Flood Awareness System (GloFAS), in: T.E. Adams, C. Gangodagamage, T.C. Pagano (Eds.), Flood Forecasting, second ed., Academic Press, 2025, pp. 299–350, https://doi.org/10.1016/B978-0-443-14009-9.00014-6.
[74] C. Cattoën, J. Conway, N. Fedaeff, D. Lagrava, P. Blackett, K. Montgomery, U. Shankar, T. Carey-Smith, S. Moore, A. Mari, T. Steinmetz, S. Dean, A national flood awareness system for ungauged catchments in complex topography: the case of development, communication and evaluation in New Zealand, J. Flood Risk Manag. 18 (1) (2025) e12864, https://doi.org/10.1111/jfr3.12864.
[75] FastFlood, FastFloodGlobal. https://fastflood.org/global/build/, 2025.
[76] Google, FloodHub. https://sites.research.google/floods/l/-36.955379009260305/175.48207861345534/10?layers=3&hide_layers=2, 2022.
[77] Copernicus, The global flood awareness system (GloFAS). https://global-flood.emergency.copernicus.eu/accounts/login/?next=/glofas-forecasting/, 2018.